Musculoskeletal Manifestations of Neurofibromatosis Type 1

Neel B. Patel[1]
Gregory Scott Stacy

OBJECTIVE. We will describe and illustrate various musculoskeletal manifestations of neurofibromatosis type 1 (NF1) encountered on imaging studies.

CONCLUSION. Because NF1 is one of the most common genetic disorders, radiologists should be familiar with its imaging manifestations.

Neurofibromatosis type 1 (NF1), also known as von Recklinghausen disease, is one of the most common genetic diseases, affecting 1 in 3000 individuals. It is an autosomal-dominant disorder due to a mutation or deletion of the *NF1* gene on chromosome 17. Neurofibromin, the gene product, acts as a tumor suppressor [1] and is important in skeletal development and growth [2]. NF1 is the most common type of neurofibromatosis and the most common of the phakomatoses, a group of congenital neurocutaneous disorders. The diagnosis is based on a variety of clinical features [3] (Table 1). NF1 is characterized by the formation of neurofibromas and abnormalities related to mesodermal dysplasia. It affects multiple organ systems, with skeletal abnormalities seen in up to 50% of patients.

Neurofibromas

The neurofibroma, a type of benign peripheral nerve sheath tumor, is the hallmark of NF1. Three varieties of neurofibromas exist: localized, diffuse, and plexiform.

Localized Neurofibromas

Most localized neurofibromas encountered in clinical practice are solitary and are seen in patients without NF1 [4]; however, in patients with NF1, localized neurofibromas represent the most common variety of neurofibroma. They usually arise during childhood and adolescence, are multiple, and tend to involve larger and deeper nerves than do neurofibromas seen in patients without NF1. Localized neurofibromas often have an elongated or fusiform shape and the affected nerve may be seen entering or exiting the mass (Fig. 1).

On MRI, localized neurofibroma lesions usually show nonspecific signal intensity and variable contrast enhancement. The classic target sign appearance, which is less common but nearly pathognomonic, is seen on T2-weighted images with high-signal-intensity myxoid material peripherally and a relatively low-signal-intensity fibrous component centrally (Fig. 2). The "reverse target" sign may be present on T1-weighted images after IV gadolinium administration; it is characterized by enhancement of the central fibrous component and a relative lack of enhancement of the surrounding myxoid component.

Diffuse Neurofibromas

Like localized neurofibromas, most diffuse neurofibromas encountered in clinical practice are solitary and are seen in patients without NF1; approximately 10% are seen in patients with NF1. Diffuse neurofibromas tend to occur primarily in children and young adults [4]. The term "diffuse neurofibroma" refers to the infiltrative nature of the tumor and does not indicate multifocality. Diffuse neurofibromas involve the skin and subcutaneous tissues, often extending to the underlying fascia, and enhance after IV gadolinium administration. Two growth patterns exist: infiltrative with a reticulated branching pattern and plaquelike with elevation of the skin and thickening of the underlying dermis [5] (Fig. 3).

Plexiform Neurofibromas

Plexiform neurofibromas, unlike localized and diffuse neurofibromas, are essentially pathognomonic of NF1, occurring in up to 40% of patients with NF1. Usually starting early in childhood, plexiform neurofibromas represent

Keywords: conventional radiography, MRI, musculoskeletal system, neurofibromatosis type 1

DOI:10.2214/AJR.11.7811

Received August 30, 2011; accepted after revision September 24, 2011.

Presented at the 2011 annual meeting of the American Roentgen Ray Society, Chicago, IL. Winner of Certificate of Merit.

[1]Both authors: Department of Radiology, University of Chicago, 5841 S Maryland Ave, MC 2026, Chicago, IL 60637. Address correspondence to N. B. Patel (neel.patel2@uchospitals.edu).

WEB
This is a Web exclusive article.

AJR 2012; 199:W99–W106

0361–803X/12/1991–W99

TABLE 1: Diagnostic Criteria for Neurofibromatosis Type 1 (NF1)

Two or more of the following must be present:
1. Six or more café au lait macules > 5 mm in diameter in prepubertal individuals or > 15 mm in diameter in postpubertal individuals
2. ≥ 2 Neurofibromas of any type or one plexiform neurofibroma
3. Freckling in the axillary or inguinal regions
4. Optic nerve glioma
5. ≥ 2 Iris Lisch nodules (iris hamartomas)
6. Sphenoid wing dysplasia or thinning of long-bone cortex, with or without pseudarthrosis
7. A first-degree relative (parent, sibling, or offspring) who meets the criteria for NF1

tortuous expansion of a long nerve segment and its branches with extension beyond the epineurium into the surrounding tissue.

Best seen on fat-suppressed T2-weighted MRI, plexiform neurofibromas present as multinodular confluent masses often with multiple target signs (Fig. 4). They can cause disfigurement and erosion of adjacent bones and respiratory or gastrointestinal obstruction from mass effect.

Malignant Peripheral Nerve Sheath Tumors

Although malignant peripheral nerve sheath tumors (MPNSTs) are relatively rare, 25–50% of cases are associated with NF1 [6]. MPNSTs may arise from any variety of neurofibroma, particularly a plexiform neurofibroma. Clinical manifestations include sudden onset of discomfort and pain at the site and new neurologic symptoms [7]. MRI findings suggesting malignant transformation include large size, peripheral enhancement pattern, perilesional edema, intramass cystic change, and heterogeneity on T1-weighted images [6] (Fig. 5). The presence of two to four of these parameters was found to have a specificity of 90% and sensitivity of 61% for detecting malignancy [6]. FDG PET shows promise as a useful adjunct to MRI for distinguishing between benign and malignant plexiform neurofibromas [8] (Fig. 6) and directs biopsy to the highest grade of the tumor.

Skeletal Manifestations of Neurofibromatosis Type 1

Discrete cutaneous or subcutaneous neurofibromas occur before puberty and may be sessile or pedunculated. They appear as circumscribed masses on radiography and on cross-sectional imaging (Fig. 7). Elephantiasis neuromatosa refers to massive enlargement of the skin and soft tissues, often associated with plexiform neurofibromas and proliferation of nerve sheath fibromyxoid tissue [9]. The resultant mass effect and pressure-induced changes may deform the underlying bone (Fig. 8). The differential diagnosis includes Proteus syndrome, hemangioma, lymphangioma, and arteriovenous malformation.

Spinal deformities occur in up to 50% of patients with NF1. Scoliosis is the most common osseous complication of NF1, affecting 21% of patients [10], and may be nondystrophic or dystrophic. Nondystrophic scoliosis has a presentation similar to that of adolescent idiopathic scoliosis, although with an earlier onset [7]; it may progress to dystrophic scoliosis, especially if the patient presents before the age of 7 years. Dystrophic scoliosis, which is characteristic of NF1, progresses more rapidly and has a poorer prognosis [7]. Kyphosis often predominates over scoliosis, with sharply angulated segments of 4–6 vertebrae (Fig. 9) associated with vertebral scalloping, neuroforaminal widening, transverse process spindling, and rib penciling [7]. Treatment is based on the degree of kyphosis, with angles of greater than 50° requiring more aggressive surgical treatment.

Dural ectasia refers to circumferential dilatation of the dural sac (Fig. 10) that may be a consequence of underlying bone weakness. It can be associated with dystrophic skeletal changes, potentially leading to spinal instability and angular deformity. Posterior vertebral scalloping is common in NF1 and is diagnosed when the depth of scalloping is greater than 3 mm in the thoracic spine or greater than 4 mm in the lumbar spine [11]. Scalloping can be associated with dural ectasia or neurofibromas [11]. The differential diagnosis of posterior vertebral body scalloping also includes several entities such as Marfan syndrome, achondroplasia, and spinal tumors.

Other dystrophic changes associated with mesodermal dysplasia include thinning of the pedicles, transverse processes, and lamina (Fig. 11) and foraminal enlargement. Neural foramina may also be expanded by dumbbell neurofibromas (Fig. 12). The differential diagnosis includes meningocele, which is usually cystic and can also occur in patients with NF1.

Rib penciling is caused by underlying mesodermal dysplasia and bony remodeling from adjacent neurofibroma. Rib penciling is present when rib width is narrower than the narrowest portion of the second rib [10] (Fig. 13).

Sphenoid dysplasia is a characteristic defect of the posterosuperior orbital wall that is attributed to mesodermal dysplasia, although a review suggests that the dysplasia may be secondary to interactions with plexiform neurofibromas early in life [12]. Findings include hypoplasia of the greater and lesser sphenoid wings along with enlargement of the middle cranial fossa [13] (Fig. 14).

The effects of mesodermal dysplasia and extrinsic pressure may result in deficient bone formation of the pectoral and pelvic girdles and of the bones of the extremities (Figs. 15–17). Findings include cortical thinning, erosive defects, periosteal proliferation, sclerosis, and cystlike lesions. Bowing and pseudarthrosis reflect mesodermal dysplasia and can occur in a variety of bones but most commonly affect the tibia [14]. Tibial bowing is typically present during the first years of life before other signs of NF1 are evident [10]. The bowing is characteristically anterolateral and tends to involve the distal diaphysis, resulting in limb shortening. Fracture typically occurs before the age of 3 years [10]. Pseudarthrosis—a false joint with abnormal movement at the site of fracture—is caused by abnormal osseous remodeling (Fig. 18). Orthopedic treatment and management of tibial pseudarthrosis are challenging and complications are common.

Well-defined, expansile lucent lesions with sclerotic margins may be seen in patients with NF1, possibly representing nonossifying fibromas (fibroxanthomas). They are classically asymptomatic, slightly expansile lesions occurring in the metaphysis of long bones that have a thin, sclerotic border with a narrow zone of transition. The presence of multiple bilaterally symmetric lower extremity nonossifying fibromas raises the possibility of underlying NF1 [15] (Fig. 19). Multiple fibroxanthoma-like lesions can also be seen in Jaffe-Campanacci syndrome, which consists of multiple nonossifying fibromas, café au lait macules, mental retardation, and hypogonadism.

Conclusion

NF1 is the most common phakomatosis and radiologists should be familiar with the imaging

manifestations of this disease. Many of the skeletal manifestations of NF1 are caused by underlying mesodermal dysplasia and nearly all parts of the skeleton and its surrounding soft tissues can be involved. Recognition of the different varieties of benign neurofibromas and of the imaging characteristics that suggest MPNST is important when interpreting imaging studies of patients with NF1.

References

1. Daston MM, Scrable H, Nordlund M, Sturbaum AK, Nissen LM, Ratner N. The protein product of the neurofibromatosis type 1 gene is expressed at highest abundance in neurons, Schwann cells, and oligodendrocytes. *Neuron* 1992; 8:415–428
2. Kolanczyk M, Kossler N, Kuhnisch J, et al. Multiple roles for neurofibromin in skeletal development and growth. *Hum Mol Genet* 2007; 16:874–886
3. [No authors listed]. Neurofibromatosis: conference statement—National Institutes of Health Consensus Development Conference. *Arch Neurol* 1988; 45:575–578
4. Murphey MD, Smith WS, Smith SE, Kransdorf MJ, Temple HT. From the archives of the AFIP: imaging of musculoskeletal neurogenic tumors—radiologic-pathologic correlation. *RadioGraphics* 1999; 19:1253–1280
5. Hassell DS, Bancroft LW, Kransdorf MJ, et al. Imaging appearance of diffuse neurofibroma. *AJR* 2008; 190:582–588
6. Wasa J, Nishida Y, Tsukushi S, et al. MRI features in the differentiation of malignant peripheral nerve sheath tumors and neurofibromas. *AJR* 2010; 194:1568–1574
7. Feldman DS, Jordan C, Fonseca L. Orthopaedic manifestations of neurofibromatosis type 1. *J Am Acad Orthop Surg* 2010; 18:346–357
8. Cardona S, Schwarzbach M, Hinz U, et al. Evaluation of F^{18}-deoxyglucose positron emission tomography (FDG-PET) to assess the nature of neurogenic tumours. *Eur J Surg Oncol* 2003; 29:536–541
9. Stevens KJ, Ludman CN, Sully L, Preston BJ. Magnetic resonance imaging of elephantiasis neuromatosa. *Skeletal Radiol* 1998; 27:696–701
10. Crawford AH, Schorry EK. Neurofibromatosis update. *J Pediatr Orthop* 2006; 26:413–423
11. Tsirikos AI, Ramachandran M, Lee J, Saifuddin A. Assessment of vertebral scalloping in neurofibromatosis type 1 with plain radiography and MRI. *Clin Radiol* 2004; 59:1009–1017
12. Jacquemin C, Bosley TM, Svedberg H. Orbit deformities in craniofacial neurofibromatosis type 1. *AJNR* 2003; 24:1678–1682
13. Binet EF, Kieffer SA, Martin SH, Peterson HO. Orbital dysplasia in neurofibromatosis. *Radiology* 1969; 93:829–833
14. Friedman JM, Birch PH. Type 1 neurofibromatosis: a descriptive analysis of the disorder in 1,728 patients. *Am J Med Genet* 1997; 70:138–143
15. Howlett DC, Farrugia MM, Ferner RE, Rankin SC. Multiple lower limb non-ossifying fibromas in siblings with neurofibromatosis. *Eur J Radiol* 1998; 26:280–283

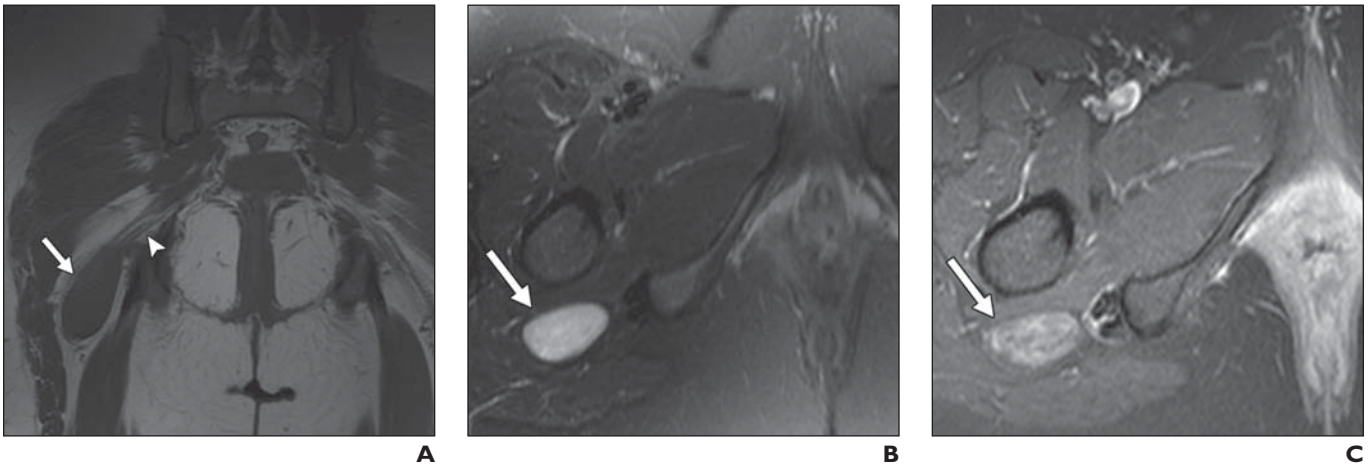

Fig. 1—37-year-old woman with solitary neurofibroma.
A, Coronal T1-weighted MR image of pelvis shows elongated mass (*arrow*) with signal intensity similar to that of muscle arising from right sciatic nerve (*arrowhead*).
B, Transverse fat-suppressed T2-weighted MR image shows mass (*arrow*) with uniform hyperintense signal.
C, Transverse fat-suppressed T1-weighted MR image obtained after IV administration of gadolinium chelate shows heterogeneous enhancement of mass (*arrow*).

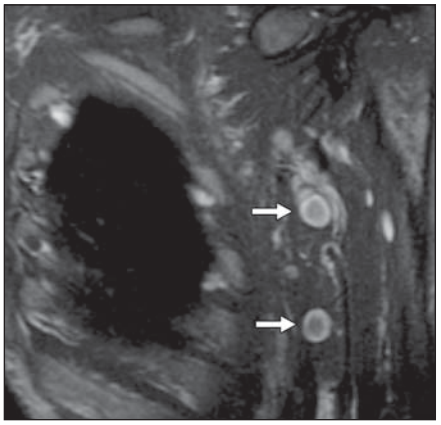

Fig. 2—35-year-old man with neurofibromatosis type 1 and shoulder pain. Coronal fat-suppressed T2-weighted MR image of left axilla shows two examples of localized neurofibromas (*arrows*) consisting of high signal intensity peripherally (myxoid component) and relatively low signal intensity centrally (fibrous component).

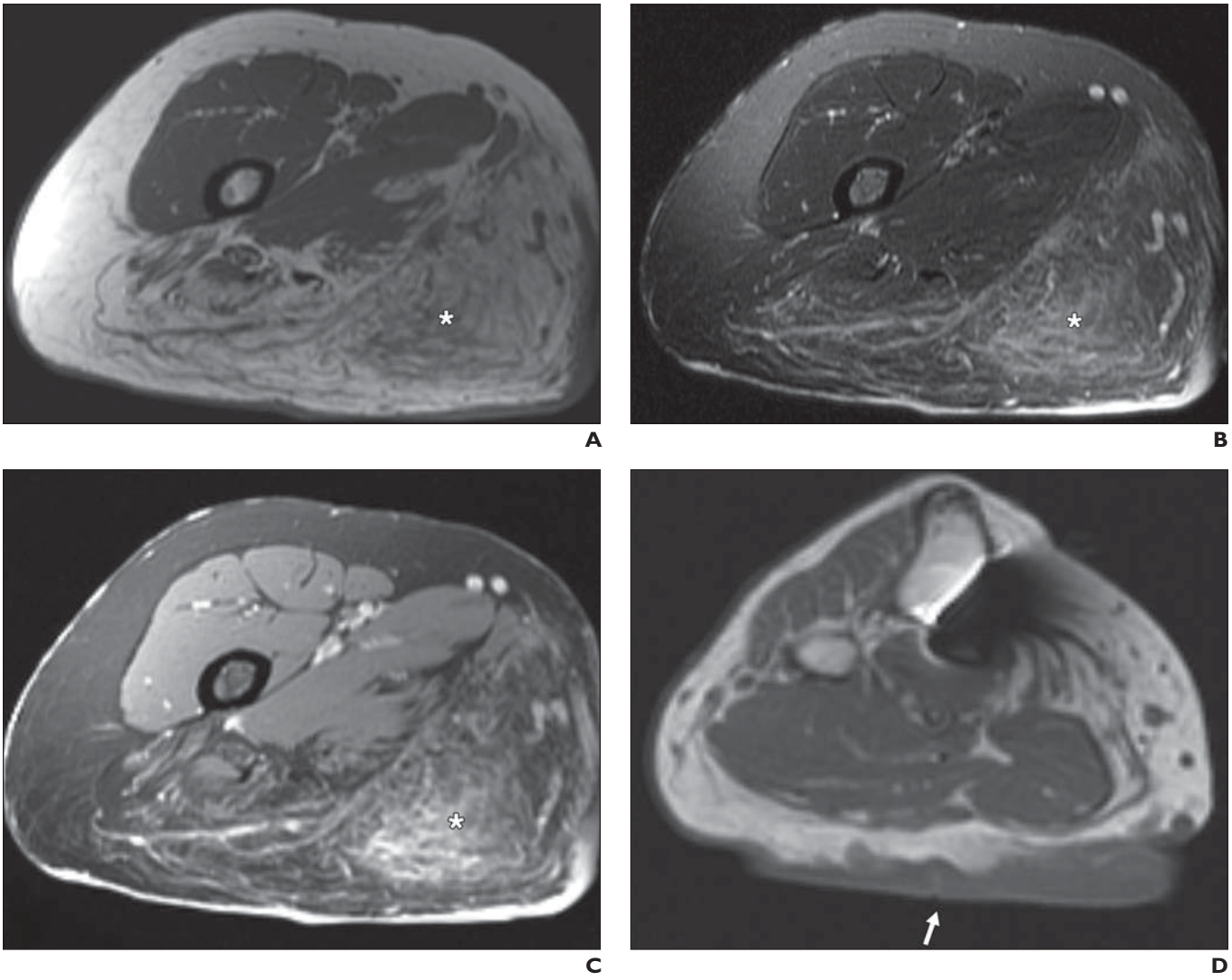

Fig. 3—47-year-old woman with neurofibromatosis type 1.
A, Transverse T1-weighted MR image of thigh shows infiltrative mass in posteromedial subcutaneous fat (*asterisk*) representing diffuse neurofibroma.
B, Transverse fat-suppressed T2-weighted MR image shows reticulated high signal intensity of mass (*asterisk*).
C, Transverse fat-suppressed T1-weighted MR image obtained after IV administration of gadolinium chelate shows enhancement of diffuse neurofibroma (*asterisk*).
D, Transverse T1-weighted MR image of upper calf shows plaquelike thickening of skin posteriorly (*arrow*) representing another diffuse neurofibroma.

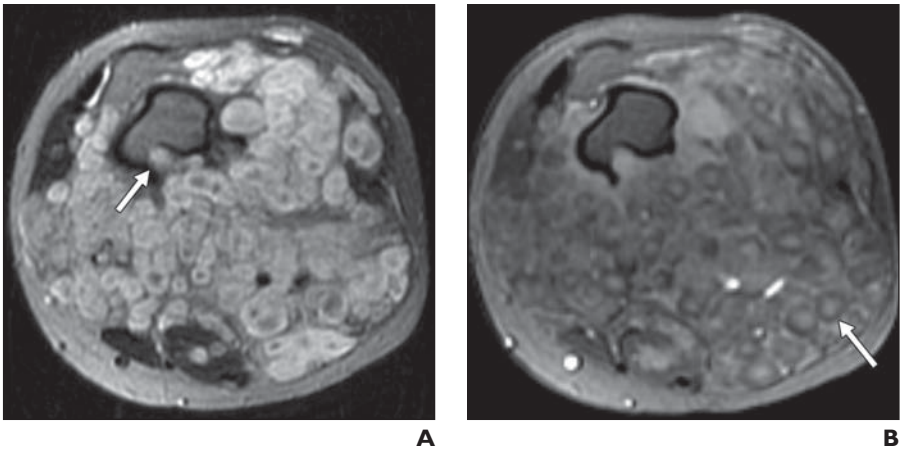

Fig. 4—17-year-old girl with neurofibromatosis type 1 and plexiform neurofibroma of left thigh.
A, Transverse T2-weighted MR image shows multinodular confluent mass with multiple target signs encasing femur. Note mass effect and endosteal scalloping along posterior aspect of femur (*arrow*).
B, Transverse fat-suppressed T1-weighted MR image obtained after IV administration of gadolinium chelate shows variable enhancement of plexiform neurofibroma with multiple "reverse target" signs (*arrow*).

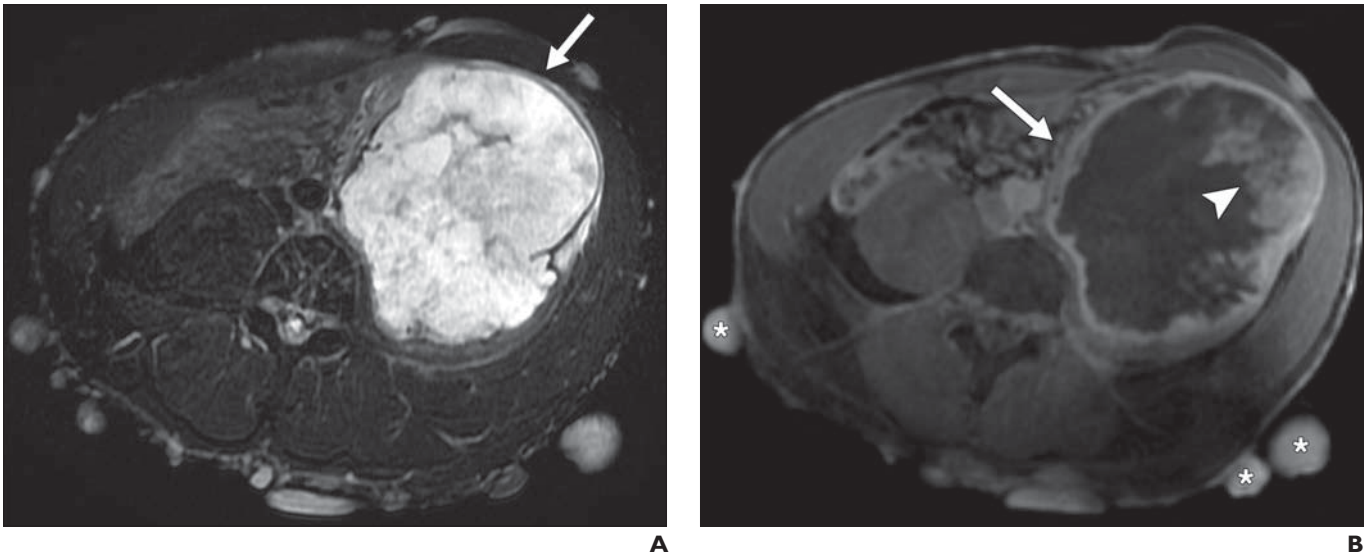

Fig. 5—45-year-old man with neurofibromatosis type 1 and malignant peripheral nerve sheath tumor.
A, Transverse fat-suppressed T2-weighted MR image shows large left lower quadrant mass (*arrow*) is exhibiting heterogeneous high signal intensity and is exerting mass effect and displacing adjacent structures.
B, Transverse fat-suppressed T1-weighted MR image obtained after IV administration of gadolinium chelate shows peripheral enhancement (*arrow*) and eccentric internal enhancement (*arrowhead*). Note homogeneously enhancing cutaneous neurofibromas (*asterisks*).

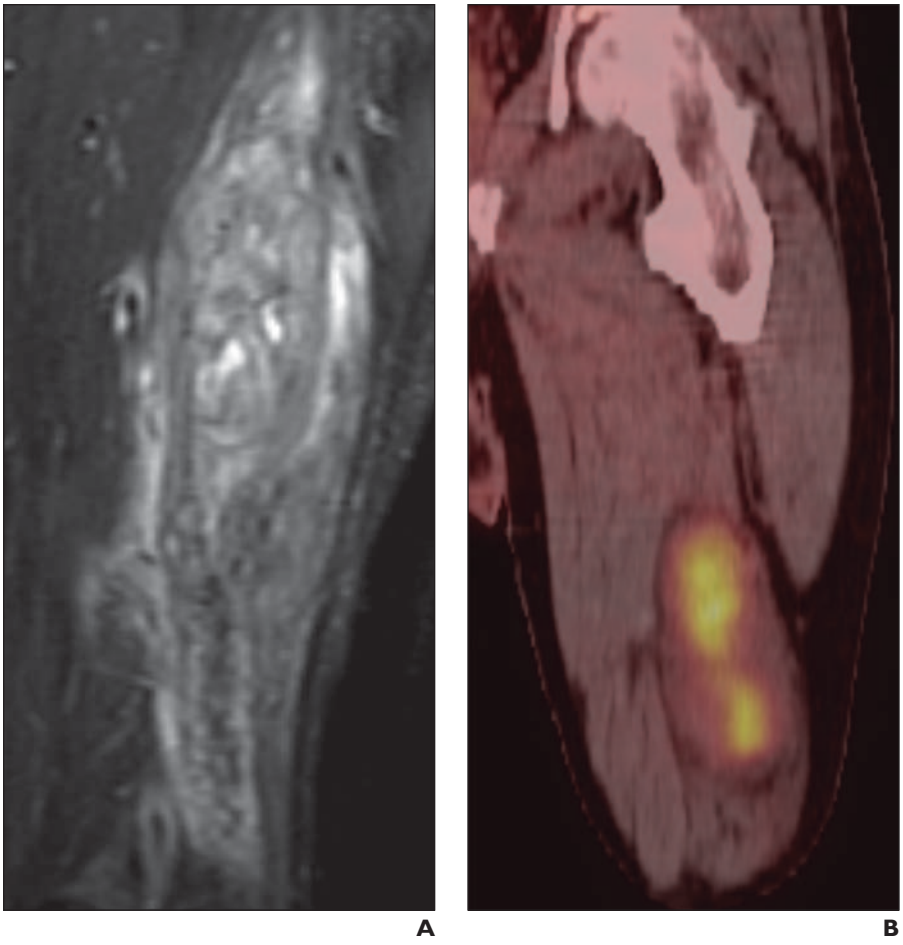

Fig. 6—48-year-old man with neurofibromatosis type 1 and malignant peripheral nerve sheath tumor (MPNST) of thigh.
A, Coronal STIR MR image of thigh shows large mass along course of sciatic nerve is exhibiting heterogeneous high signal intensity.
B, Coronal fused FDG PET/CT image shows intense heterogeneous uptake within posterior thigh corresponding to MPNST.

Fig. 7—54-year-old woman with neurofibromatosis type 1 and cutaneous neurofibromas. Posteroanterior radiograph of left hand shows multiple cutaneous soft-tissue masses (*arrows*) representing neurofibromas.

Fig. 8—47-year-old man with neurofibromatosis type 1 and elephantiasis neuromatosa. Posteroanterior radiograph of left hand shows diffuse soft-tissue hypertrophy; note also enlargement and mild cortical irregularity of thumb phalanges.

Fig. 9—30-year-old woman with neurofibromatosis type 1 and dystrophic scoliosis. Sagittal reformatted CT image of thoracic spine shows dystrophic scoliosis with sharply angulated kyphosis and posterior spinal fixation rods.

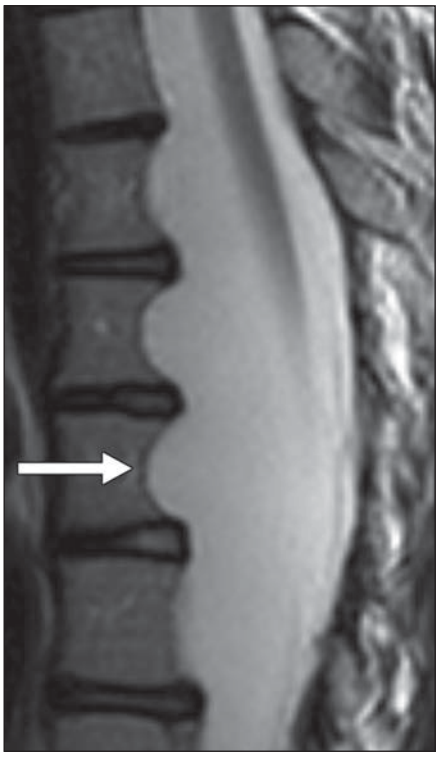

Fig. 10—19-year-old woman with neurofibromatosis type 1 and dural ectasia. Sagittal T2-weighted MR image of thoracic spine shows posterior vertebral scalloping (*arrow*) along with dural ectasia.

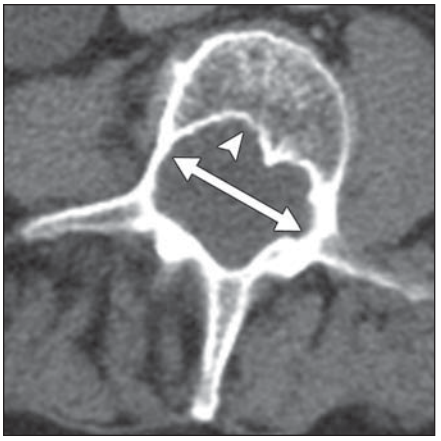

Fig. 11—65-year-old man with neurofibromatosis type 1 and dystrophic spinal deformity. Transverse CT image of lumbar spine shows thinning of pedicles, widening of interpedicular distance (*double-headed arrow*), and posterior vertebral body scalloping (*arrowhead*). ←

Fig. 12—24-year-old man with neurofibromatosis type 1. Transverse T2-weighted MR image of spine shows dumbbell neurofibroma (*asterisk*) expanding neural foramen and invading spinal canal. →

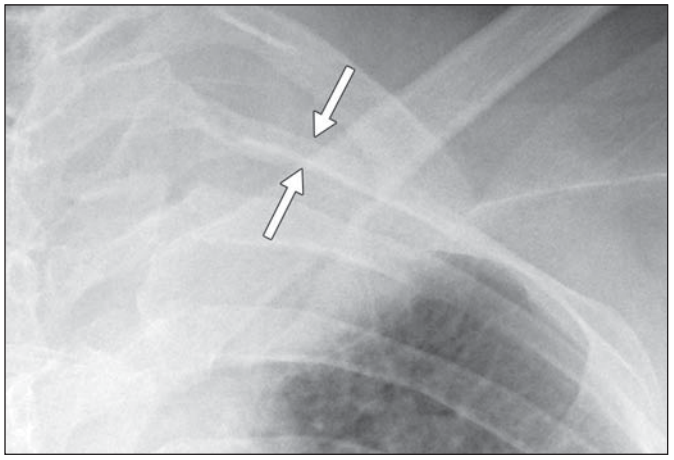

Fig. 13—24-year-old man with neurofibromatosis type 1. Anteroposterior radiograph of ribs shows thinning of second rib posteriorly, "ribbon rib" appearance (*arrows*).

A

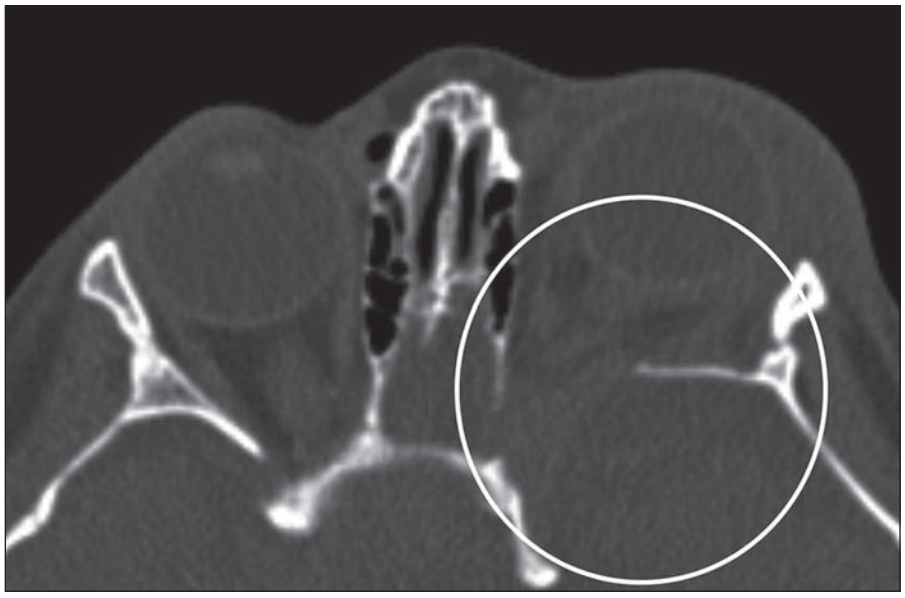

B

Fig. 14—6-year-old boy with neurofibromatosis type 1 and sphenoid dysplasia.
A, Three-dimensional reconstruction of CT image of skull shows enlargement of left orbit and hypoplasia of left sphenoid.
B, Transverse CT image shows enlargement of superior orbital fissure and middle cranial fossa (*circle*). Enlargement of superior and inferior orbital fissures due to plexiform neurofibromas infiltrating trigeminal nerve can also occur in absence of sphenoid dysplasia [12].

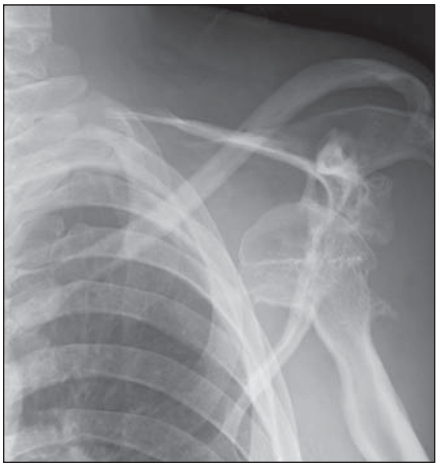

Fig. 15—20-year-old man with neurofibromatosis type 1 and mesodermal dysplasia resulting in bone deformity. Anteroposterior radiograph of left shoulder shows dysmorphic glenoid, thinning and deformity of clavicle and scapula, and dislocated proximal humerus.

Fig. 16—30-year-old man with neurofibromatosis type 1. Anteroposterior radiograph of knee shows cortical thinning and multiple lucencies in proximal fibula and mild scalloping of tibial cortex due to mesodermal dysplasia.

Fig. 17—58-year-old woman with neurofibromatosis type 1. Anteroposterior radiograph of right hip shows dysplastic acetabulum with deformity of femoral head and thinning of proximal femur.

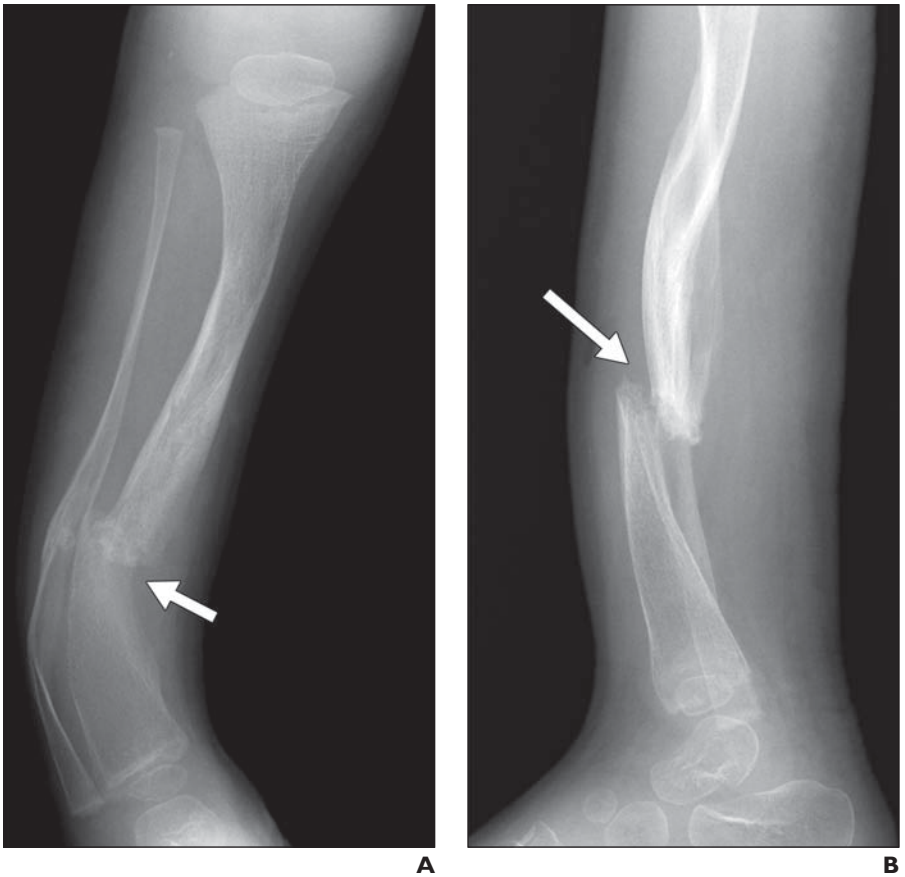

Fig. 18—20-month-old girl with neurofibromatosis type 1 and pseudarthrosis of tibia.
A, Anteroposterior radiograph of right leg shows anterolateral bowing (*arrow*) of distal diaphysis of tibia and fibula.
B, Lateral radiograph shows pseudarthrosis of tibia with anterior displacement of distal tibial fragment (*arrow*).

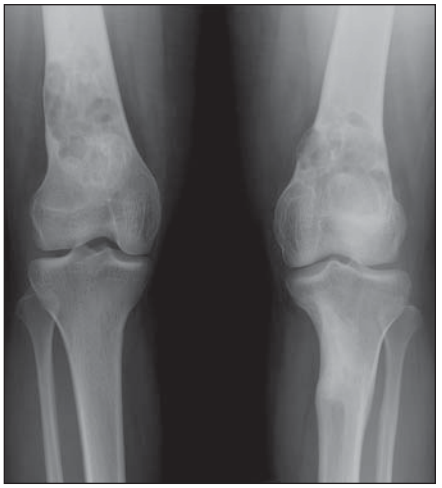

Fig. 19—23-year-old woman with neurofibromatosis type 1. Anteroposterior radiograph of knees shows bilateral sharply marginated lucent lesions with sclerotic margins in both distal femurs; these findings are suggestive of fibroxanthomas. Sclerosis and mild deformity of left proximal tibia were caused by prior curettage of lesion with healed pathologic fracture.